Journal of Materials Chemistry B

ROYAL SOCIETY OF CHEMISTRY

REVIEW

View Article Online
View Journal | View Issue

Cite this: J. Mater. Chem. B, 2023, 11, 11483

Recent advancements in Mg-based micromotors for biomedical and environmental applications

Yue Wang,[a] Boyu Qin,*[e] Sihan Gao,[a] Xuanchun Wang,[a] Hongyue Zhang*[b] and Zhiguang Wu *[acd]

Received 8th October 2023,
Accepted 18th November 2023

DOI: 10.1039/d3tb02339g

rsc.li/materials-b

Synthetic micro/nanomotors have attracted considerable attention due to their promising potential in the field of biomedicine. Despite their great potential, major micromotors require chemical fuels or complex devices to generate external physical fields for propulsion. Therefore, for future practical medical and environmental applications, Mg-based micromotors that exhibit water-powered movement and thus eliminate the need for toxic fuels, and that display optimal biocompatibility and biodegradability, are attracting attention. In this review, we summarized the recent microarchitectural design of Mg-based micromotors for biomedical applications. We also highlight the mechanism for realizing their water-powered motility. Furthermore, recent biomedical and environmental applications of Mg-based micromotors are introduced. We envision that advanced Mg-based micromotors will have a profound impact in biomedicine.

1. Introduction

With the advancements in micro- and nano-technologies, micro/nanomotors that can convert their own energy or energy from the local environment into mechanical energy[1–3] and perform movements under the control of external fields have been proposed.[4–8] Micromotors can perform various tasks that are difficult for macroscale robots to complete, such as minimally invasive surgery,[9] targeted drug delivery,[10,11] bioimaging,[12,13] biosensing,[14,15] and cell transportation,[16–18] and they therefore have great application prospects in the field of biomedicine. Due to biological barriers preventing the transport of therapeutics, in conventional drug delivery, drug molecules are distributed freely throughout the body, and these molecules generally do not precisely reach the desired location. Therefore, the efficiency of drug delivery methods needs to be improved.[19] An improvement in the efficiency can be realized through the use of micro/nanomotors. Various drugs can be loaded on micromotors for active delivery, and Mg can react

[a] School of Medicine and Health, Harbin Institute of Technology, Harbin 150001, China. E-mail: zhiguangwu@hit.edu.cn
[b] Laboratory for Space Environment and Physical Sciences, Harbin Institute of Technology, Harbin 150001, China. E-mail: hongyuezhang@hit.edu.cn
[c] State Key Laboratory of Robotics and System, Harbin Institute of Technology, Harbin 150001, China
[d] Key Laboratory of Microsystems and Microstructures Manufacturing (Ministry of Education), Harbin Institute of Technology, Harbin 150001, China
[e] Department of Oncology, The Fifth Medical Center of Chinese PLA General Hospital, Beijing 100039, China. E-mail: qpm2017@126.com

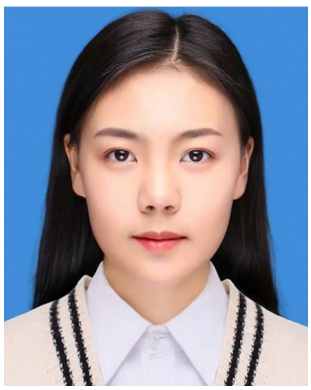

Yue Wang

Yue Wang obtained her Bachelor of Engineering degree in 2022 from Harbin University of Science and Technology, China. Currently, she is a master's student studying at the School of Chemistry and Chemical Engineering, Harbin Institute of Technology, China. Her research interest is Mg-based Janus micromotors.

Boyu Qin

Boyu Qin obtained an MSc in Cancers from the University College London (UCL) and worked initially as an associate staff in the cancer institute of UCL. Currently, she is a doctor in the department of oncology of Chinese people's liberation army general hospital. Her current research interests include cancer targeted therapy, cancer immunotherapy, tumor immune microenvironment, nanomedicine, big data and artificial intelligence in precision oncology.

with the local environment to produce active H_2 that can remove hydroxyl free radicals in the organism, further improving the therapeutic effect.[20,21] In addition, the self-stirring effect generated by the self-driven micromotors in a fluid also promotes bacteria removal from that environment[22] and improves detection efficiency in biosensing applications.[23]

Thus, because of the versatility of micromotors, they are promising for applications in several fields, including the biomedical field. Therefore, the development of micromotors with biocompatibility, degradability, and motility is of considerable importance. Fig. 1 is a summary of the structure, motion, and related applications of Mg-based micromotors.

However, in practical applications, micro/nanomotors have many limitations in terms of their microscopic characteristics, especially the Reynolds number (Re) of micro-/nanomotors. The motility of micromotors depends on the radius of micromotors (R), the density of fluids (ρ), the speed of micromotors (V), and the viscosity of the fluid (η); Re is given by

$$\mathrm{Re} = \frac{\rho R V}{\eta} \approx \frac{\text{intertial forces}}{\text{viscous forces}}$$

With the development of micromotors with increasingly smaller sizes, the Re in water or biological fluids has also decreased. With decreasing Re, the influence of viscous forces in the fluids becomes greater than that of inertial forces; the disturbance of the flow rate in the fluids will be decreased by the viscous force, and the macro driving mode will no longer be applicable on the micro level which is a major challenge for propelling micromotors. Subsequently, studying how to carry out a long-term efficient motion has become a problem that needs to be addressed.[35,36]

Early chemically driven micromotors were propelled by the decomposition of H_2O_2 with noble metals (such as Pt) to produce O_2 that drove micromotors by the recoil force generated by O_2 bubbles. As early as 2002, catalytically propelled motors on a centimetre scale were realized.[37] In 2004, Sen *et al.* proposed a rod-shaped Pt/Au/Ni nanomotor in which the Pt

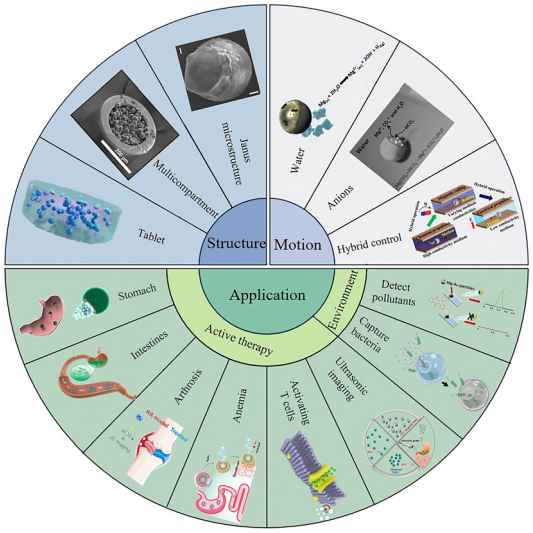

Fig. 1 Schematic summary of the structure, movement, and applications of Mg-based micromotors. Janus microstructure. Reproduced with permission. Copyright 2020, Elsevier Ltd. All rights reserved.[24] Multicompartment. Reproduced with permission. Copyright 2023, The Authors. Small published by Wiley-VCH GmbH.[25] Tablet. Reproduced with permission. Copyright 2022, American Chemical Society.[26] Water. Reproduced with permission. Copyright 2017, American Chemical Society.[22] Anions. Reproduced with permission. Copyright 2013, Wiley-VCH Verlag GmbH & Co. KGaA, Weinheim.[27] Hybrid control. Reproduced with permission. Copyright 2022, American Chemical Society[28] Stomach. Reproduced with permission. Copyright 2017, Springer Nature.[29] Intestines. Reproduced with permission. Copyright 2022, American Chemical Society.[26] Arthrosis. Reproduced with permission. Copyright 2021, American Chemical Society.[21] Anemia. Reproduced with permission. Copyright 2019, American Chemical Society.[30] Activating T cells. Reproduced with permission. Copyright 2020, Elsevier Ltd. All rights reserved.[31] Ultrasonic imaging. Reproduced with permission. Copyright 2021, Elsevier Ltd. All rights reserved.[32] Capture bacteria. Reproduced with permission. Copyright 2019, Wiley-VCH Verlag GmbH & Co. KGaA, Weinheim.[33] Detect pollutants. Reproduced with permission. Copyright 2016, American Chemical Society.[34]

Hongyue Zhang

Hongyue Zhang received her PhD in 2021 from Harbin Institute of Technology, China. She is an assistant professor currently working at the Laboratory for Space Environment and Physical Sciences, Harbin Institute of Technology, China. Her research interests include biohybrid swimming micro/nanorobots, especially cell-based nanorobots for biomedical applications.

Zhiguang Wu

Zhiguang Wu obtained his PhD from Harbin Institute of Technology, China in 2015, then he anticipated Prof. Peer Fischer group as a postdoc researcher under Alexander von Humboldt Foundation research fellow in the Max Plank Institute for Intelligence System, Stuttgart, Germany. Subsequently he is studying as a postdoc researcher in Prof. Wei Gao's group at California Institute of Technology. Currently, he is a professor at the Harbin Institute of Technology. In 2019, he was selected "Innovators under 35 China" in the MIT Technology Review. His research interest focuses on the development of micro-/nano-robots for biomedicine.

segment can catalyse the generation of O_2 bubbles from H_2O_2 in the solution and propel micromotors.[38] In addition, Jänis *et al.* synthesized poly(3,4-ethylenedioxythiophene) (PEDOT)/MnO_2 tubular micromotors through template-assisted deposition. The catalytic activity and rate when MnO_2 acted as the catalyst were higher to a certain extent than that when Pt was the catalyst.[39] With the further development of micro- and nano-technologies, Janus micromotors with various physical and chemical properties, such as optical, magnetic, and acoustic properties, have been developed to achieve functional diversity and collaboration. For example, Cai and Ren *et al.* reported a photo-responsive bismuth iodide (BiOI) micromotor whose motion can be controlled by its response to light at different wavelengths.[40] For ultrasound-driven micromotors, mainly using the piezoelectric effect of materials, Iino *et al.* found that the asymmetrical micromotor can create different sound pressures using ultrasound to make the motor rotate.[41] Magnetic and electric fields also regulate the speed and direction of micromotors with magnetic or conductive materials. However, these micromotors usually require an external control platform, and the operation process is complicated. Chemically driven micromotors are propelled by the medium or carried by the ''fuel'' itself, relying on the chemical gradient of the ''fuel'' to achieve propulsion, and the locally available chemical energy is converted into a driving force. This has the advantages of simplicity and high speed.

Although H_2O_2 as a ''fuel'' can effectively propel micromotors, this method is not suitable for a wide range of applications *in vivo* due to the strong oxidation and biological toxicity of H_2O_2.[27] In order to avoid the side effects of H_2O_2 *in vivo*, Mano *et al.* proposed a bioelectrochemically driven micromotor that is driven by the reaction between glucose and O_2, and showed that the energy generated in the bioelectrochemical reaction can be directly converted into the mechanical power for propulsion.[42] Wilson *et al.* successfully prepared a biocompatible enzyme-driven Janus micromotor based on hollow mesoporous silica nanoparticles (HMSNPs). The micromotor is powered by a biocatalytic reaction of three different enzyme/fuel combinations (catalase/H_2O_2, urease/urea, and GO_x/glucose). These micromotors can be loaded with both hydrophilic and hydrophobic drugs and are promising for drug delivery applications.[43] However, few suitable enzymes have been identified and the performance of these micromotors is limited by the local environment; finally, researchers have designed Janus micromotors with water as the fuel.[44,45]

Mg is an essential trace element and the main intracellular earth-metal cation that plays an important role in mental function. For example, Mg is important for maintaining human cardiovascular health[46] and for promoting the regeneration of human nerve and bone cells.[47] Moreover, Mg can significantly improve the HDL-cholesterol levels of patients with diabetes,[48] improve the health of patients with non-alcoholic fatty liver disease,[49] and reduce the risk of strokes.[50] Studies reported that insulin can enhance cellular Mg uptake among patients with diabetes, and Mg intake is correlated to the degree of hyperglycaemia.[51] A person deficient in Mg will present with health issues such as cardiometabolic disease,[52] moderate tension-type headaches,[53] and alcohol-related liver injury.[54] Currently, Mg is widely used in bone scaffolds in the body.[55] Mg is not only crucial for bodily functions but also has a very high reactivity: micrometre-scale Mg can easily react with water to produce $Mg(OH)_2$ and H_2. The generated H_2 bubbles can propel micromotors. The $Mg(OH)_2$ can be etched by salt ions in a physiological environment, to carry out continuous bubble-driven motion. The reaction rate of Mg can also be increased by heating or by introducing metals such as Al, Zn, Sr, and Mn, to increase the current corrosion. Furthermore, the motion of Mg-based micromotors can be regulated *via* reactions of Mg between solution and other ions so that Mg-based micromotors can complete various transportation tasks in complex fluid environments.[56]

In this paper, in order to clarify the development and potential applications of Mg-based micromotors, the unique properties of Mg-based micromotors, a variety of preparation methods, and various motility types are discussed. In addition, the use of Mg-based micromotors for *in vivo* therapy and environmental remediation and biosensing is introduced. Finally, the potential applications and existing challenges of Mg-based micromotors are discussed.

2. Architectonics for Mg-based micromotors

The chemically propelled micro/nanomotors must have an asymmetrical structure to create the local asymmetry field to offer the driving force. Researchers have proposed Janus micromotors composed of asymmetric materials that have an asymmetric structure.[69] Janus micromotors have two different regions, one that is anisotropic in composition and another with a large specific surface area. These micromotors exhibit not only a sufficient number of modification sites but also a single-direction propulsion force.[36]

2.1 Janus microstructure

The micromotors with the Janus structure have a unique design that combines two different components in a single unit. Thus, Mg-based Janus micromotors exhibit a combination of different properties that impart new analytical capabilities to the micromotors. To fabricate the Janus structure of Mg-based micromotors, Tu *et al.* dispersed Mg microspheres on a glass sheet and then coated the surface of the Mg microspheres with poly(lactic-*co*-glycolic acid) (PLGA) containing doxorubicin hydrochloride (DOX). This was followed by drying, and then, the Mg/PLGA@DOX Janus micromotors were lightly scratched off the glass sheet and collected (Fig. 2a).[24] The bottom-up multilayer modification method is one of the most commonly used strategies for preparing Mg-based Janus micromotors. By employing this strategy, simple and easily modified substances are imparted with multifunctional layers, such as a temperature-responsive layer, a pH-responsive layer, and a layer of loaded drugs.[30,31,57] Mg microparticles were dispersed onto

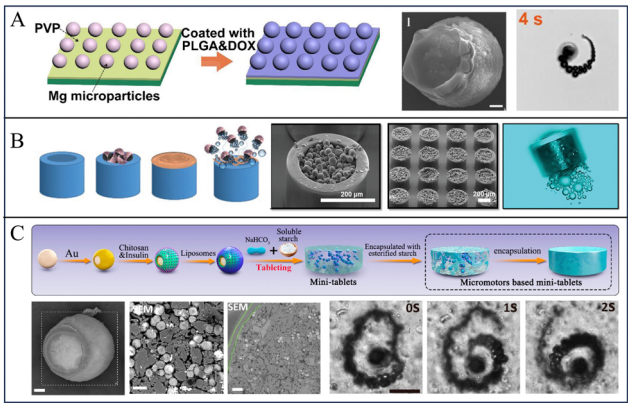

Fig. 2 Various structures of Mg-based micromotors. (A) Mg-based Janus sphere micromotors. Reproduced with permission. Copyright 2020, Elsevier Ltd. All rights reserved.[24] (B) Mg-based micromotors for intestinal tract targeted nesting inside microcontainers. Reproduced with permission. Copyright 2023, The Authors. Small published by Wiley-VCH GmbH.[25] (C) An oral Mg-based micromotor tablet. Reproduced with permission. Copyright 2022, American Chemical Society.[26]

glass slides or polymethyl methacrylate (PMMA) to form a monolayer, and then, the metal layer was deposited, thereby modifying the polymer. Because part of Mg is blocked by glass or PMMA, the metal layer and the polymer cannot be attached to this part, resulting in an asymmetric structure. If Mg microspheres are dispersed on the PMMA, the micromotors can be collected by dissolving the PMMA film.[58,59] Wang *et al.* and Zhang *et al.* coated red blood cell (RBC) membranes on the surface of Mg-based micromotors to realize micromotors with great biocompatibility and the ability to simulate cell motion. A layer of Mg microparticles was dispersed on a parafilm, and then, Au and alginate (ALG) were deposited on the surface of Mg. Finally, RBC membranes were coated onto the AuNP/ALG-covered surface.[57]

The Janus structure can also be prepared using asymmetric evaporation of a water-in-oil (w/o) emulsion. For example, the PABA-modified GODs were dissolved in an aqueous solution containing surfactants, and then, Pt and Fe_3O_4 nanoparticles were dissolved in chloroform; the resulting two solutions were evenly mixed to obtain a w/o emulsion. Because the w/o interface energy reduces spontaneously when the solution evaporates, the asymmetric deposition of nanoparticles was realized.[60] Due to its simple preparation and easy multi-functional modification, the Janus structure is the most common form for bubble-ejection.

2.2 Multicompartment structure

To improve the penetration capability and cargo protection, one strategy is to nest Mg-based micromotors into multicompartment microdevices. For example, Maric *et al.* proposed a cascade device that loads Mg-based micromotors (Fig. 2b). The cascade devices were prepared by dispersing Mg microspheres on top of a 2-inch single-side polished silicon wafer, and by then depositing an Au layer by ion sputtering deposition. Subsequently, paracetamol was dissolved in ethanol and mixed with Mg/Au micromotors for 18 h to coat the micromotors with the drug and lid. To prepare multicompartment containers, a nanoscale layer of Ti and Au was deposited on a 4-inch silicon substrate by physical vapor deposition to promote the detachment of a single microcontainer after micromotor loading. The substrate was cut into millimetre-scale chips. This was followed by filling of the gap of the microcontainer with polydimethylsiloxane (PDMS) to prevent micromotors from being loaded into the gap, and then, the micromotors were loaded onto each chip. Finally, PDMS was carefully removed with tweezers to obtain the microscale containers full of micromotors.[25]

Wang and Zhang *et al.* prepared tubular Mg-based micromotors using a polycarbonate (PC) film by using the template-assisted deposition technique. First, a layer of Au was deposited by sputtering on one side of the PC film as the working electrode, and then, PEDOT/Au microtubules were deposited on the film by electrochemical deposition. Next, 1–5 μm Mg spheres were loaded into the microtubules by vacuum infiltration. Finally, the PC film was dissolved with methylene chloride to obtain tubular micromotors. Furthermore, to protect the micromotors from reaction before reaching the intestine, the surface of the micromotors were coated with an enteric coating. The resultant micromotors can deliver drugs precisely *via* dissolution of the enteric coating to activate the propulsion and prolong the retention time of the drug in the tissue.[61] Moreover, they also used a similar method to prepare Zn-based multicompartment micromotors.[62]

2.3 Tablet

To improve the usage of Mg-based micromotors for clinical translation, Mg-based micromotors were incorporated into a tablet for oral administration. For instance, Wang and Zhang *et al.* reported a microstirring pill for oral drug delivery: first, a single layer of TiO_2 was deposited on Mg microspheres by sputtering. Then, lactose and maltose were mixed with drugs and micromotors. Finally, the resulting mixture was mixed with 75% ethanol solution to form a paste that was pressed to form the tablets. The Mg-based-micromotor tablet delivery system displays a high efficiency in drug delivery *via* oral administration. The investigation in both murine and porcine models illustrate that this tablet enhances the bioavailability of drug payloads *in vivo*.[63] Subsequently, to improve the bioavailability and reduce the blood sugar levels of patients with diabetes, a similar method was used to prepare self-stirring tablets loaded with metformin.[64]

Liu, Peng, and Tu *et al.* adopted the hydrophobic modification of natural starch by acetic anhydride, washed and removed pyridine and unreacted acetic anhydride to obtain esterified starch, and then dried and pulverized the esterified starch; then, they prepared insulin-loaded Mg/Au-CHI Janus micromotors by bottom-up deposition and coating with a Mg monolayer. Finally, esterified starch and micromotors were mixed and then pressed into tablets (Fig. 2c).[26] These tablets with a self-stirring capability display improved drug delivery efficiency and enhanced drug absorption after gastrointestinal delivery *in vivo*.

3. Motion

The chemical propulsion of micromotors usually requires an asymmetric field, and this type of propulsion can be categorized as self-electrophoresis, self-diffusiophoresis, and bubble-ejection.[65] Self-electrophoresis is led by uneven proton distribution that reduces or oxidizes around the micromotors, and self-diffusiophoresis enables motility through an asymmetric concentration gradient field. However, self-electrophoresis and self-diffusiophoresis can usually be driven well in salt-rich environments, because it is limited by ion concentrations. Because of the low solubility of the gas in solution and the surface tension in liquid, when micromotors react with the local environment to produce gas, a succession of bubbles are generated at the opening of the micromotors. Bubble-ejection micromotors can thus generate microjets when bubbles grow and collapse at the opening and propel micromotors by the recoil force from microjets.[65,66] The details regarding the propulsion of Mg-based micromotors are given in Table 1. The displacement of each micromotor is the superposition of the radius of each bubble, so the size and frequency of bubbles are the key factors affecting the speed of the micromotor.

The progress of Mg-based micromotors is expressed as follows:

$$\text{Motility: } Mg + 2H^+ = Mg^{2+} + H_2\uparrow$$

$$\text{Form passivation: } Mg^{2+} + 2OH^- = Mg(OH)_2\downarrow$$

$$\text{Etch passivation: } Mg(OH)_2\downarrow + 2HCO_3^- = Mg^{2+} + 2CO_3^{2-} + 2H_2O$$

Guan *et al.* reported the motion of Mg-based micromotors *via* a Mg–water reaction. In water, the reaction of Mg with water generates $Mg(OH)_2$ and H_2, and $Mg(OH)_2$ on the exposed Mg surface impedes the further progress of the reaction, so the rapid removal of this passivation layer is necessary. Therefore, Guan *et al.* dissolved $Mg(OH)_2$ in an aqueous solution of sodium $NaHCO_3$ because HCO_3^- reacts with insoluble $Mg(OH)_2$ to form soluble CO_3^{2-}, so Mg can react with water and generate H_2 bubbles. Subsequently, they proposed the motion of Mg-based micromotors in simulated body fluid (SBF) and blood plasma. They considered using anions (such as Cl^- and HCO_3^-) in blood plasma to improve the motion of micromotors, and found that the pit corrosion induced by Cl^- and the buffering effect of SBF and blood

Table 1 The motion of Mg-based micromotors

Material	Size	Medium	Speed	Ref.
Therapy				
Mg, Au	~27	Simulated gastric fluid	~90	68
Mg, Au, PEDOT	Length 15, diameter 5	Gastric and intestinal fluid	~60	61
Mg, Au	~20	Gastric fluid	~60	67
Mg, TiO_2, PLGA, Fe, Se	~20	Simulated intestinal fluid	~119	30
Mg, Au, RBC, ALG	~20	0.08 M NaCl	~165	57
Mg, TiO_2, RBC, CHI	~20	Intestinal fluid	~150	69
Mg, TiO_2	~25	Simulated gastric fluid, 1.2% Triton X-100, 37 °C	~350	64
Mg, TiO_2	~25	Simulated intestinal fluid, 1.2% Triton X-100, 37 °C	~180	64
Mg, Au, CHI, liposomes	~25	Simulated intestinal solution, mucin	~80	26
Mg, Au, crosslinked SU-8	Diameter 300; height 240	2 M NaCl, 0.34% Triton X-100	~17	25
Mg, Au	~24	2 M NaCl, 0.34% Triton X-100	~55	25
Mg, PLGA, ALG, CHI, anti-CD3	~20	0.5 M $NaHCO_3$, 0.2 wt% SDS	~42	31
Mg, Au, TiO_2, PLGA, CHI	~20	PBS (pH = 5)	~27	73
Mg, PLGA	~27	Simulated body fluid	~57	24
Mg, PLGA, HA hydrogel	~21	Simulate synovial fluid	~40	21
Mg, PLGA	~24	Artificial cerebrospinal fluid	~51	20
Mg, TiO_2	~20	Simulated gastric fluid	~190	72
Mg, TiO_2	~10	Simulated intestinal fluid	~62	72
Mg, TiO_2, macrophage	~20	Simulated gastric fluid	~136	72
Mg, TiO_2, macrophage	~10	Simulated intestinal fluid	~19	72
Environmental remediation				
Mg, Au, Ti, Ni	~30	0.3 M NaCl	~90	45
Mg, Au, Ti, Ni	~30	3 M NaCl	~300	45
Mg, Au, TiO_2	~20	Seawater (0.54 M NaCl)	~110	74
Mg, Au, PLGA, ALG, CHI	~20	Drinking water	~36	75
Mg, PLGA, ALG, CHI	~20	Seawater	~72	75
Mg, Ag, Fe, Au	~15	Water pH 6, 2% Tween-20	~12	22
Biosensing				
Mg, Au	~20	Milk	~108	34
Mg, Au	~20	Water	~296	34
Mg, Au	~20	Whiskey	~223	34
Mg, Au	~20	Serum	~40	34
Mg, Pt	~30	HS/PBS-FcMeOH, 1 mM glucose	~80	76
Mg, Fe_3O_4	~25	PBS	~53	58
Mg, Fe_3O_4	~25	Siluted serum	~30	58
Mg, Fe_3O_4	~25	Diluted blood	~28	58

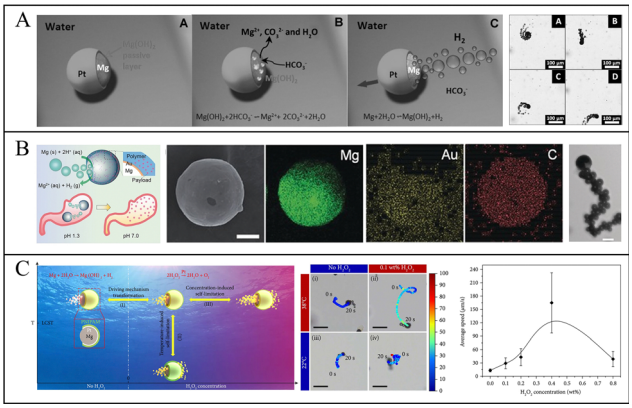

Fig. 3 Motion of Mg-based micromotors. (A) Etched $Mg(OH)_2$ on the surface of Mg-based Janus micromotors by HCO_3^-. Reproduced with permission. Copyright 2013, Wiley-VCH Verlag GmbH & Co. KGaA, Weinheim.[27] (B) Acid-responsive Mg-based micromotors moving in simulated gastric fluid. Reproduced with permission. Copyright 2017, Wiley-VCH Verlag GmbH & Co. KGaA, Weinheim.[67] (C) Mg-based Janus micromotors moving in response to variations in temperature and H_2O_2 concentration. Reproduced with permission. Copyright 2020, Kang Xiong *et al.*[70]

plasma increased the speed of micromotors (Fig. 3a).[27,44] Moreover, Wang *et al.* also reported that the motion of Mg-based micromotors depended on the Cl^- concentration, so increasing the Cl^- concentration could effectively improve the speed of micromotors. For example, when the concentration of NaCl in the medium was increased from 0.3 M to 3 M, the speed of micromotors could be increased from 90 μm s^{-1} to 300 μm s^{-1}.[45] To further stabilize the generated bubbles in order to improve the driving efficiency, a minority surfactant, such as SDS,[31] Triton X-100,[64] and Tween-20,[22] is added to the reaction medium. Finally, thermal energy can also improve the motion of micromotors: as the temperature rises, the rate of bubble generation increases, thus increasing the speed of the micromotors.

Physiological conditions, especially the gastric acid environment that has abundant H^+ and anions, can effectively improve the motion of micromotors. Further study of the motion of micromotors in biological fluids showed that Mg-based micromotors exhibit efficient motion in simulated gastric fluid (Fig. 3b)[67,68] and simulated intestinal fluid.[26,69] Wang and Zhang *et al.* studied the speed of micromotors in simulated gastric and simulated intestinal fluids, and the speed of the micromotors was as high as 350 μm s^{-1} in simulated gastric fluid with a low pH and decreased to 180 μm s^{-1} in simulated intestinal fluid with higher pH.[64]

However, the control of the direction of micromotors is difficult: a single-drive can no longer propel the micromotor to complete complicated tasks. To control the motility of micromotors, field-controlled particles were induced based on chemically driven micromotors. Wang *et al.* loaded micromotors with magnetic nanoparticles by ion beam sputtering to control the direction of the micromotors by using an external magnetic field. They deposited a Ni layer on the micromotors so the micromotors could move to the target area and be recovered through magnetic field control.[45] This method not only controls the micromotor in the complex environment, but also improves the motility of the micromotor after the fuel is exhausted. Later, Mei *et al.* also designed a tubular micromotor with a catalytic Pt layer and a magnetic Ni layer; the micromotor can be continuously propelled by H_2 bubbles generated by the reaction of the Pt layer and H_2O_2, and the direction of micromotors can be controlled by using a magnetic field.[71] The size of the micromotor can also affect the speed: Mei *et al.* also demonstrated that when the size of micromotors range from 10 to 15 μm, the average speed of micromotors was ~190 μm s^{-1}, and when the size was 20–25 μm, the average speed was ~63 μm s^{-1} in the simulated gastric fluid.[72]

Guan *et al.* proposed micromotor-movement control using variations in the temperature and H_2O_2 concentration (Fig. 3c). In a solution containing $NaHCO_3$, Mg reacts with water to generate H_2, and $Mg(OH)_2$ on the surface can be continuously etched by HCO_3^-. When H_2O_2 is added to the solution, the catalytic reaction of H_2O_2 and Pt is more likely to occur than the reaction between Mg and H_2O. Therefore, the driving mode of Mg-based micromotors will change, the H_2O_2 decomposition reaction is the main reaction, effectively extending the driving life of the micromotor. The temperature-sensitive poly (*N*-isopropyl acrylamide) (PNIPAM) hydrogel layers deposited on Mg-based micromotors exist in a state of hydrophilic expansion when the temperature is lower than the lower critical solution temperature (LCST), so H_2O_2 has a high diffusion constant. When the temperature is lowered to the point where the concentration of H_2O_2 penetrating PNIPAM is high enough to generate bubbles, bubbles will be generated on both sides of the micromotors, so the speed of the micromotors will reduce and they may even hover in place.[70]

Enzyme-driven chemical drive methods are also important. Unlike traditional fuels, enzymes are biocompatible, making enzyme-powered micromotors valuable in the biomedical field.[77] Wu's group designed a tubular DNA assembly enzyme-powered micro-motor capable of reaching a movement speed exceeding 450 μm s^{-1} through an enzymatic reaction at a concentration of 5% wt H_2O_2.[78] Sánchez's group designed a porous micromotor built from a metal–organic framework (MOF) and powered by enzymatic reactions. Catalase was loaded in the porous structure of the MOF, and H_2O_2 was used as fuel to power the micromotor through the O_2 bubbles generated by the enzymatic reactions.[79] To further enhance the motility of enzyme-powered micromotors, Sánchez's group discovered that commonly used enzymes were not pure enough. After purifying the enzyme, they found that the micromotor loaded with purified urease achieved about 2.5 times the speed of the motor loaded with unpurified urease.[80]

4. Biocompatibility

Mg-based micromotors have great biocompatibility: other common metal micromotors usually do not degrade adequately in the body, but because Mg-based micromotors are driven by Mg

as the fuel, the Mg core will be exhausted and retained in the body in the form of ions. Mg is a common mineral in the human body, and the Mg^{2+} concentration is the second largest of cations in cells. Moreover, Mg^{2+} is a cofactor and is indispensable for energy and nucleic acid synthesis. Mg^{2+} can bind electrostatically to negatively charged groups in membranes, proteins, and nucleic acids.[51] Additionally, Mg has been approved by the U.S. Food and Drug Administration (FDA) for *in vivo* use,[81] and it is widely used in biological implant applications.[82]

The polymers deposited on the surface of Mg-based micromotors, such as PLGA, PVP, and Eudragit L100-55, also exhibit good degradability and biocompatibility in the body.

Wang and Zhang *et al.* investigated gastrointestinal drug delivery in mice; the gastrointestinal tract of mice was observed with hematoxylin and eosin (H&E) staining after 24 h. The results were compared with those for a control group, and no significant changes in the epithelial structure of the gastrointestinal tract and no signs of inflammation were found on the mucosa and submucosa.[61]

Similarly, Peng and Tu *et al.* performed H&E staining of the gastrointestinal tissues of mice 1 day and 7 days after drug delivery. A comparison of the results for the control group and of the group administered the micromotors showed that the intestinal tissue structure did not change significantly one day after administration, and the colonic mucosa remained smooth without any damage after continuous administration for 7 days.

Thus, the Mg-based micromotors have good biocompatibility and biosafety.[26]

5. Applications

Mg-based micromotors exhibit a wide range of biomedical applications, including the transportation of drugs, antigens, and cells, which play important roles in therapy. Moreover, micromotors can effectively enhance the fluid mass transfer process in the environment, accelerating environmental remediation and biosensing.

5.1. Active therapy

Conventional passive treatment methods lack precision and controllability. Due to their motility and ease of functionalization, micromotors enable drug delivery to the target area and then release drugs, thereby improving the retention period in the body.[29,30,57] In addition, the H_2 generated during the driving process of Mg-based micromotors can also be used as an active substance for hydrogen therapy.[20,21,24,83] Thus, by combining hydrogen therapy,[73] Mg-based micromotors provide an optimal pathway for active therapy *in vivo*.

5.1.1. Targeted delivery. Conventional passive drug delivery has the limitations of low targeting accuracy, short retention time *in vivo*, and low delivery efficiency, but micromotors show great potential for targeted drug delivery. Wang and Zhang *et al.* applied micromotors *in vivo* for the first time. They deposited a single layer of Mg over glass, and they applied a TiO_2 coating over the Mg surface *via* atomic layer deposition. The resulting micromotors can be loaded with clarithromycin and used to treat *Helicobacter pylori* infection (Fig. 4a); this method can effectively reduce the bacterial load *in vivo*.[29] To ensure that most of the drug is released in the stomach, Liu and Li *et al.* coated the surface of micromotors with pH-responsive *Eudragit®L100-55* to complete the co-delivery of amoxicillin and clarithromycin for treating the infection due to *Helicobacter pylori*.[68] Guan *et al.* also proposed the use of Mg/Pt-PNIPAM Janus micromotors for temperature-controlled release of the loaded drug. After they coated micromotors with a layer of temperature-responsive PNIPAM, they loaded FITC in PNIPAM and confirmed that the rate of FITC release was much higher at 37 °C than at 20 °C. These results indicate that PNIPAM can effectively change the drug release behaviour of micromotors at different temperatures, and this method is promising for realizing controllable drug release.[44]

To prevent the drug from being released prematurely in the stomach, Wang and Zhang *et al.* introduced an enteric coating on the surface of the micromotor so that the motor can smoothly pass through the stomach and then into the intestine: they deposited PEDOT/Au microtubules on a porous carbonate membrane, and then, loaded Mg into the tubules, thus preparing tubular Mg-based micromotors (Fig. 4b). Enteric Mg micromotors are 25% less likely to stay in the stomach compared with uncoated micromotors. Their data verified that both the enteric coating and self-driving feature are crucial for accurate delivery and drug retention.[61] They also found that the micromotor can neutralize the stomach acid and adjust the gastric pH to neutral in less than 20 minutes. Compared with the traditional method, Mg-based micromotors can temporarily change the local environment without affecting the other functions of the local environment. The effect of traditional

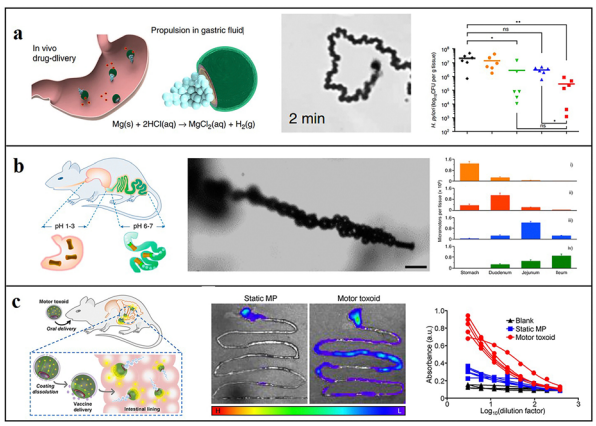

Fig. 4 Application of Mg-based micromotors for active targeted delivery. (A) Clarithromycin-loaded Mg-based micromotor for treating *Helicobacter pylori* infection. Reproduced with permission. Copyright 2017, Springer Nature.[29] (B) Tubular Mg-based micromotors with pH-responsive retention in the gastrointestinal tract. Reproduced with permission. Copyright 2016, American Chemical Society.[61] (C) Mg-based micromotors used for active antigen delivery to the gastrointestinal tract in order to induce mucosal immunity. Reproduced with permission. Copyright 2019, American Chemical Society.[69]

inhibitors is eliminated, and the release of drug loads can be triggered by the active regulation of the local environment.[67] A similar method in which Fe and Se are loaded on self-driven Mg-based micromotors coated with an enteric membrane can also enhance the delivery and absorption of minerals in the intestine, to treat anaemia.[30]

Although micromotors have many applications in biotherapy, most materials used are metals, which have poor degradability *in vivo* and inadequate biocompatibility. To improve the biocompatibility of micromotors, Wang and Zhang *et al.* proposed Mg-based Janus micromotors with cell membrane functionalization. These are composed of Mg, RBC membranes, Au nanoparticles, and ALG to mimic the movement of natural cells. These micromotors can attract, capture, and neutralize toxins *in vivo* through the cell simulation function of RBCs.[57] Subsequently, they used RBCs to effectively fix and neutralize the toxin, and loaded them on Mg-based micromotors, then coated chitosan and enteric-soluble polymer on the outermost layer (Fig. 4c). In response to changes in the gastrointestinal pH value, micromotors can effectively deliver the toxin to the intestine. Compared with traditional vaccine methods, the active delivery of oral vaccines can greatly improve immunogenicity, antigenicity, and safety, and it can be widely used for the safe load delivery of a variety of antigens by regulating the composition of the load.[69]

The biocompatibility, degradability, and safety of micromotors *in vivo* can be significantly improved by using cell membranes and biocompatible materials such as PLGA, CHI, and ALG, thus potentially enabling further applications of micromotors *in vivo*. However, the problem of how real-time monitoring of micromotors can be realized persists. To solve this, Wu and Li *et al.* proposed an intestinal micromotor combined with photoacoustic computed tomography (PACT). Mg-based Janus micromotors were encapsulated in a capsule and released drugs in the intestine through near-infrared light irradiation. Then, PACT was used for real-time monitoring. These micromotors can not only be monitored in real-time but also prolong the retention time of the drug in the intestine because they are self-driven.[84]

For the convenience for oral administration, the Mg-based micromotors were integrated into tablets. Wang and Zhang *et al.* prepared Mg-based micromotor tablets through the bottom-up multilayer modification of metformin, lactose, and maltose. These tablets exhibit a self-stirring capability because of the motility of the micromotors, and this improves the interaction of the tablet with local biological fluids and enables accelerated drug transport and release. Experimental results show that the rate of reduction in the postprandial blood sugar levels realized by using self-stirring metformin tablets was higher than that achieved *via* the traditional delivery of metformin.[64] To improve the resistance of oral insulin to the harsh digestive environment, Liu, Peng, and Tu *et al.* proposed the oral delivery of insulin system *via* tablets of insulin-loaded Mg micromotors and auxiliary materials with subsequent esterified by starch encapsulation; by using these tablets, blood sugar control for more than 5 h was realized.[26] To increase the speed of micromotors and enhance the penetration of micromotors into the gastrointestinal mucous membrane of organisms, Maric *et al.* proposed a cascading device that nested Mg-based Janus micromotors in a microcontainer for drug loading and transportation. The advantage of this microcontainer is that it can provide the best conditions for spraying the micromotors into the mucus layer that is not readily penetrated by the microcontainer. In addition, the rate of propulsion of micromotors enclosed within the microcontainers through the mucous membrane was faster than that of single Janus micromotors.[25]

The micromotor described above only exhibits rapid self-driving in a single-component, unvarying, uniform medium, but biological environments are usually complex with considerable differences in the local pH and the ions contained in different tissue parts. Therefore, in these complex environments, a single propulsion driver may be insufficient for the micromotor to complete necessary tasks, and the Mg-based micromotor can be stopped when the Mg core is almost consumed. To solve this problem, Wang and Yossifon *et al.* proposed a triple-engine hybrid micromotor with electric and magnetic fields. Under the conditions of a low pH, the fluid conductivity is high, and the micromotors are mainly chemically driven; on the other hand, they are mainly electrically driven in the medium with a low conductivity and the transition area is dominated by magnetic rolling. At a low electric field frequency, the motor can capture cells at the opening of Janus micromotors. In addition, the drug contained in the micromotor shell can be delivered to these captured cells, and with the increase in the electric field frequency, the captured cells can be released. The single-cell-capture capability of these micromotors enables local electroporation and transfection of drugs and genes.[28]

In addition to drug delivery, micromotors can be used in immunotherapy. Peng and Tu *et al.* proposed a PLGA/ALG/CHI-coated Mg-based micromotor system with an anti-CD3 load for antigen presentation; this can trigger Ca^{2+} channels to activate T cells and further trigger immune signals to clear pathogens and malignant cells.[31] To enhance the effect of tumour immunotherapy, Wang and Zhang *et al.* prepared a Mg-based micromotor coated with a bacterial outer membrane and used the interaction of Mg-based micromotors with water in solid tumours to destroy the surrounding tumour tissue. The bacterial outer membrane vesicles carry a series of immune-stimulating molecules, which can cause the biological immune response. This method combines the destruction of tumour tissue with biological stimulation and effectively alleviates the effect of cancer.[73]

5.1.2 Hydrogen therapy. Excessive reactive oxygen species (ROS) and free radicals are the main causes of ischemic stroke, inflammation, and other problems. In 2007, it was discovered that H_2 molecules can selectively remove hydroxyl radicals ($^{\bullet}OH$) during oxidative stress and inflammation, while preserving other ROS, such as H_2O_2, superoxide, and NO.[83] Hydrogen therapy has become a common treatment method in medicine. In addition to targeted delivery, the H_2 generated by the

reaction between the Mg core and the local environment also provides the active ingredient for H_2 therapy. Furthermore, the H_2 production time and amount exhibited by micromotors are higher than those observed when traditional H_2-rich solutions or gas are used.

Guan *et al.* adopted a modified Stöber method to coat Mg-based Janus micromotors with mesoporous SiO_2 nanoshells and adjusted the thickness of the nanoshell by adjusting the proportion of tetraethyl orthosilicate (TEOS) to control the H_2 release rate (Fig. 5a). Under physiological conditions, micromotors can produce H_2 efficiently for a long time to remove •OH and protect cells from oxidative damage, and cells treated with the micromotors show a higher activity. Moreover, the SiO_2 shell can be easily modified with other substances, and this opens up new avenues for potential applications involving intelligent H_2 reservoirs.[85] Liu, Hu, Peng, and Tu *et al.* treated tumour cells with Mg-based micromotors loaded with DOX. The motility characteristics of the micromotors indicated a higher drug delivery efficiency, and the locally generated H_2 effectively improved the sensitivity of tumour cells toward chemotherapy drugs.[24] They also prepared Mg-based Janus micromotors by an asymmetric coating of Mg with hyaluronic acid (HA) hydrogel and PLGA, and then injected micromotors into the knee-joint under ultrasound guidance (Fig. 5b). The H_2 produced by the reaction of the Mg core with the local environment can not only propel micromotors but also decrease the ROS content in cells and clear inflammation. This method has shown remarkable therapeutic effects in treating arthritis damage and inhibiting arthritis.[21] These micromotors can also solve stoke, injecting micromotors into the lateral ventricle of middle cerebral artery occlusion (MCAO) rats, by using the self-drive of the micromotors and the generation of active H_2, the infarct volume in the brain of the rats was effectively reduced.

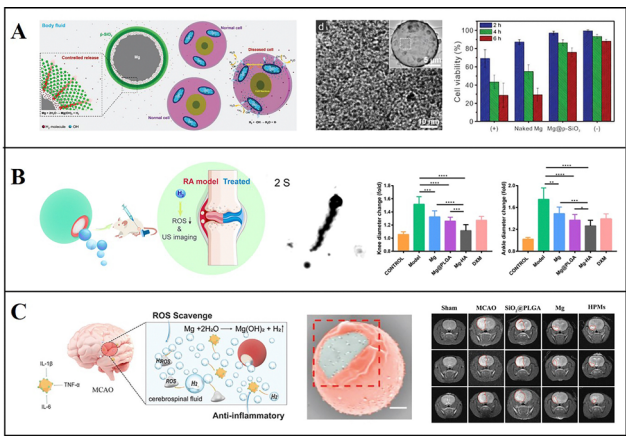

Fig. 5 Mg-based micromotors for hydrogen therapy. (A) Mg-based Janus micromotors for removal of hydroxyl free radicals (•OH). Reproduced with permission. Copyright 2018, WILEY-VCH Verlag GmbH & Co. KGaA, Weinheim.[85] (B) Mg-based Janus micromotors used in hydrogen therapy for treating rheumatoid arthritis. Reproduced with permission. Copyright 2021, American Chemical Society.[21] (C) Mg-based Janus micromotors used in hydrogen therapy for treating acute ischemic stroke. Reproduced with permission. Copyright 2021, Wiley-VCH GmbH.[20]

By using this method the spatial learning and memory ability of the rats were greatly improved[20] (Fig. 5c).

In addition to the treatment of diseases, the bubbles continuously generated by micromotors under physiological conditions can be employed as contrast enhancers under ultrasound guidance. Li and Li *et al.* coated the surface of the Mg-based micromotor with Ni and controlled the micromotor to reach the target environment by using a magnetic field. Under the influence of the ionic environment, the micromotor was chemically driven and generated numerous bubbles. The bubbles gathered under ultrasound guidance, which can effectively enhance the contrast of ultrasonic imaging and imaging effect. This method has great application potential in the field of medical imaging.[32]

5.2 Environmental remediation

Mg-based Janus micromotors can be readily modified, so they can also be widely employed in environmental remediation. Through modification of the surface of micromotors by using bactericidal substances and chemical attractants, bacteria can be captured and eliminated with the self-driven micromotors, to enhance the local environmental mass transfer and to improve the speed and efficiency of sterilization.

Wang *et al.* proposed a Mg/Ti/Ni/Au Janus micromotor that is coated with Ti, Ni, and Au metal layers on a Mg monolayer, and uses galvanic corrosion and pitting corrosion in seawater to react $Mg(OH)_2$ on the surface of micromotors, so as to promote the reaction between Mg and water producing bubbles for promotion, which can eliminate the requirement for external fuel. The Ni layer on the surface of the micromotor can be used for magnetic guidance, and through the control of an external magnetic field, the micromotor can approach, capture, and transport motor oil droplets in seawater, thus realizing environmental remediation.[45] In addition to carrying pollutants out of the environment, they remove insoluble matters by modifying the photocatalyst and sterilizing through the ROS generated from Mg. They coated the Mg monolayer with TiO_2 containing Au nanoparticles to prepare Mg-based Janus micromotors, which can be self-driven to complete environmental remediation (Fig. 6a). The TiO_2 coating can remove hard-to-decompose bis(4-nitrophenyl)phosphate chemical warfare agents under the action of photocatalysis. ROS generated by the interaction of the Mg core with water can destroy *Bacillus anthracis* spores and thus display a bactericidal effect.[74] Dong *et al.* also killed *Escherichia coli* in the environment by using Mg-based Janus micromotors modified with Ag nanoparticles and found that the bactericidal effect of this method was nine times that of static methods.[86] Moreover, Wang *et al.* assembled a monolayer of meso-2,3-dimercaptosuccinic acid (DMSA) on the surface of Janus micromotors, and used these to effectively chelate heavy metal ions from polluted water media. The Zn, Cd, and Pb removal rates using these micromotors reached 100%.[87]

To improve the biodegradability and recyclability of micromotors for water sterilization, Wang *et al.* proposed a simple and environmentally friendly method of coating Mg micromotors with

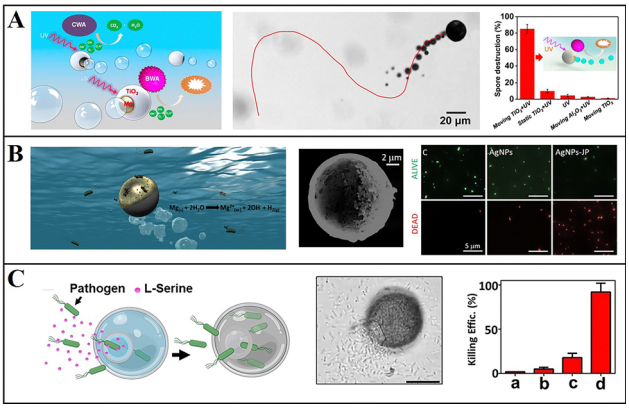

Fig. 6 Mg-based micromotors for environmental remediation. (A) Mg-based Janus micromotors for photocatalytic degradation of *Bacillus globigii* spores. Reproduced with permission. Copyright 2014, American Chemical Society.[74] (B) AgNP-modified Mg-based Janus micromotors to kill bacteria by releasing Ag ions. Reproduced with permission. Copyright 2017, American Chemical Society.[22] (C) L-Serine-modified Mg-based Janus micromotors for attraction, trapping, and destruction of pathogens. Reproduced with permission. Copyright 2019, Wiley-VCH Verlag GmbH & Co. KGaA, Weinheim.[33]

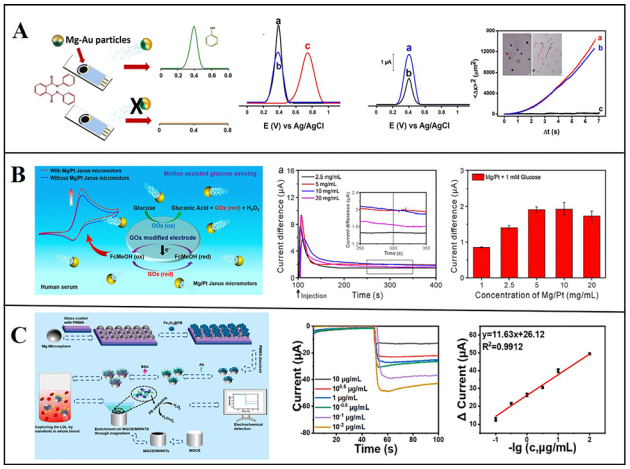

Fig. 7 Mg-based Janus micromotors in biosensing. (A) Mg-based Janus micromotors for the detection of organic pollutants in food and biological samples. Reproduced with permission. Copyright 2016,[34] American Chemical Society. (B) Mg-based Janus micromotors used for the detection of glucose in human serum. Reproduced with permission. Copyright 2019, American Chemical Society.[76] (C) Mg-based Janus micromotors for electrochemical sensing of oxidized low-density lipoprotein (Ox-LDL) in human blood. Reproduced with permission. Copyright 2022 Elsevier B.V. All rights reserved.[58]

highly biodegradable CHI, ALG, and PLGA. Because of the motility characteristics of micromotors, they can almost completely kill bacteria within 10 min.[75] Sánchez *et al.* synthesized Mg/Au/Fe Janus micromotors modified with Ag nanoparticles, in which the magnetic Fe layer is used for magnetic guidance and recovery of micromotors (Fig. 6b). When micromotors are in contact with water, H_2 bubbles are generated and drive the movement of micromotors, increasing the contact opportunity between modified Ag ions and bacteria. This method involving these micromotors has a higher sterilization efficiency than the static method and can effectively kill more than 80% of *E. coli*.[22]

To further improve the efficiency of micromotors in capturing and killing bacteria, Wang *et al.* proposed an onion-like multifunctional microtrap with Mg as the self-driven core and with Ag nanoparticles and the inducer L-serine, to realize the attraction, capture, and destruction of pathogens (Fig. 6c). This micromotor enhances the accumulation and capture of *E. coli* within the trap through the chemical inducer L-serine and their killing *via* the release of Ag nanoparticles.[33] These studies on the use of micromotors for environmental remediation and water purification present an economical and environmentally friendly solution.

5.3 Biosensing

Conventional detection methods require complex sample processing, and due to the limitation of detection methods, such as the mass transfer of liquid samples being slow and uneven, result in a long detection time and low sensitivity. With the motility of micromotors and the generation of bubbles, the mass transfer of liquid samples can be greatly improved, so the liquid samples can become more uniform, thereby improving the detection accuracy. Furthermore, micromotors can directly convert some substances that are difficult to detect, such as non-electrically active substances, into electrochemically active substances and then detect them *via* electrochemical detection.

Wang *et al.* reported micromotor-assisted printable sensor strips that enable efficient electrochemical measurements: they deposited Ni and Au on a Mg monolayer by ion beam sputtering deposition to prepare Mg/Ni/Au Janus micromotors that quickly convert undetectable paraoxon into detectable electroactive *p*-nitrophenol. The Ni layer can fix micromotors on the sensing strip by magnetically constraining them, thus preventing the micromotors from moving to the electrode region. Through the interaction of Mg and water, bubbles are generated and enable effective fluid transport, and the fluid near the anchor points is significantly improved.[23] Subsequently, Jurado-Sánchez and Escarpa *et al.* deposited an Au layer on Mg micromotors to prepare Mg/Au Janus micromotors that are capable of efficient degradation and detection of persistent organic pollutants in biological samples. The self-stirring improves the analysis signal, and the non-electroactive diphenyl phthalate (DPP) was quickly converted into electroactive phenol by the hydroxyl which was generated by the reaction of Mg with water, and the electrical signal was detected on the electrode (Fig. 7a). Thus, DPP can be directly detected in food and biological samples without any sample handling, and carbohydrates and dopamine can be detected with different electrodes.[34]

The fast self-driving speed of micromotors can enhance the mass transfer of fluids. To improve the speed and accuracy of biosensing, Guan *et al.* used Mg/Pt Janus micromotors for the electrochemical detection of glucose in human serum (Fig. 7b). They found that the current increases with the number of micromotors, and this method involving micromotors is faster and more accurate than static detection is, confirming its great

Table 2 Advantages and disadvantages of Mg-based micromotors in different applications

	Advantage	Disadvantage
Biomedical	High drug delivery efficiency; Prolong the retention time of drugs in the body; Provide active substances for auxiliary hydrogen therapy hydrogen therapy;	Difficult for precise direction control;
Analytical	Simple operation process; Low cost; Fast detection speed and high precision;	Limited life;
Environment remediation	High precision; Good self-degradability; Recyclable	Limited life;

application prospects in biosensing.[76] Furthermore, Mou and Zhou *et al.* prepared Mg–Fe_3O_4@PB@Ab@BSA Janus micromotors to detect oxidized low-density lipoprotein (Ox-LDL) in human blood by electrochemical sensing. After the Mg cores are depleted, Fe_3O_4 can capture, collect, and detect Ox-LDL on a magnetic glass electrode modified with multi-walled carbon nanotubes. It can detect the Ox-LDL in a whole blood solution at the range from 1×10^{-2} to 10 μg mL^{-1}, with high sensitivity, good reproducibility, and a linear response (Fig. 7c).[58] Wan and Shen *et al.* prepared aldehyde-functionalized Mg-based Janus micromotors using PMMA as the substrate and an aldehyde–amine condensation reaction to modify Fe_3O_4/polydopamine/anti-epithelial cell adhesion molecule (EpCAM). Tumour cells were also captured and detected by magnetic glass electrodes. This work presents a reliable method for the early detection of cancer and prompt initiation of its treatment.[59]

6. Conclusions

This review presents a comprehensive overview of the progress in research on Mg-based micromotors in recent years. The preparation and motion control of various Mg-based micromotors have been discussed. These Mg-based micromotors are suitable for therapy, biosensing, environmental remediation, and other applications, and these methods exhibit lower costs, simple procedures, and high efficiencies. Mg-based micromotors are expected to be used as drug carriers for tumour treatment, especially stomach tumours because the gastric acid environment is extremely favourable for driving the micromotors, and rapid analysis and detection of biological samples by using micromotors is also expected. Furthermore, in sewage treatment plants, micromotors can replace traditional chemical agents to eliminate and recover bacteria and harmful substances. The advantages and disadvantages of Mg-based micromotors in various applications are summarized in Table 2.

Despite their various advantages and capabilities, Mg-based micromotors still need to be improved for practical applications. First, the lifetime of Mg-based micromotors is limited: when the Mg core is exhausted, the micromotor is no longer self-driven. Although H_2 produced in the process of micromotor driving is beneficial to the human body, when the amount produced in the body is very high, adverse side effects may be experienced, so the amount of Mg-based micromotors cannot exceed a certain limit. Finally, direction control has always been a difficult challenge for chemically driven micromotors because factors including external field control and the introduction of magnetic particles and light-responsive particles are usually needed. Therefore, a further study of motility, biocompatibility and degradability becomes necessary. These challenges limit the practical and commercial applications of Mg-based micromotors. However, with continuous innovations in materials and technologies, Mg-based micromotors are expected to become important for diverse biomedical and environmental applications.

Author contributions

Y. W. summarized wrote the manuscript. B. Q. supervised the studies. S. G. and X. W. collected and organized relevant literature and materials. H. Z. checked the manuscript. Z. W. conceived the project. All authors reviewed the manuscript.

Conflicts of interest

There are no conflicts to declare.

Acknowledgements

This work is financially supported by the National Natural Science Foundation of China (21972035 and 52375565), the Interdisciplinary Research Foundation of HIT (IR2021112), and the State Key Laboratory of Robotics (2019-O02).

Notes and references

1 C. Zhou, N. J. Suematsu, Y. Peng, Q. Wang, X. Chen, Y. Gao and W. Wang, *ACS Nano*, 2020, **14**, 5360–5370.
2 F. Mou, Q. Xie, J. Liu, S. Che, L. Bahmane, M. You and J. Guan, *Natl. Sci. Rev.*, 2021, **8**, nwab066.
3 F. Wong and A. Sen, *ACS Nano*, 2016, **10**, 7172–7179.
4 Y. Hou, H. Wang, R. Fu, X. Wang, J. Yu, S. Zhang, Q. Huang, Y. Sun and T. Fukuda, *Lab Chip*, 2023, **23**, 848–868.
5 H. Zhang, Z. Li, C. Gao, X. Fan, Y. Pang, T. Li, Z. Wu, H. Xie and Q. He, *Sci Robot*, 2021, **6**, eaaz9519.
6 Y. Gao, F. Wei, Y. Chao and L. Yao, *Biomed. Microdevices*, 2021, **23**, 52.
7 L. Ren, W. Wang and T. E. Mallouk, *Acc. Chem. Res.*, 2018, **51**, 1948–1956.

8 L. Xu, D. Gong, N. Celi, J. Xu, D. Zhang and J. Cai, *Appl. Surf. Sci.*, 2022, **579**, 152165.
9 W. Xi, A. A. Solovev, A. N. Ananth, D. H. Gracias, S. Sanchez and O. G. Schmidt, *Nanoscale*, 2013, **5**, 1294–1297.
10 M. Luo, Y. Feng, T. Wang and J. Guan, *Adv. Funct. Mater.*, 2018, **28**, 1706100.
11 R. Lin, W. Yu, X. Chen and H. Gao, *Adv. Healthcare Mater.*, 2021, **10**, e2001212.
12 Q. Wang, K. F. Chan, K. Schweizer, X. Du, D. Jin, S. C. H. Yu, B. J. Nelson and L. Zhang, *Sci. Adv.*, 2021, **7**, eabe5914.
13 D. Vilela, U. Cossio, J. Parmar, A. M. Martinez-Villacorta, V. Gomez-Vallejo, J. Llop and S. Sanchez, *ACS Nano*, 2018, **12**, 1220–1227.
14 Q. Wang, T. Shi, M. Wan, J. Wei, F. Wang and C. Mao, *J. Mater. Chem. B*, 2021, **9**, 283–294.
15 Y. Hu, W. Liu and Y. Sun, *Adv. Funct. Mater.*, 2021, **32**, 2109181.
16 M. Amouzadeh Tabrizi, M. Shamsipur, R. Saber and S. Sarkar, *Biosens. Bioelectron.*, 2018, **110**, 141–146.
17 M. S. Draz, N. K. Lakshminaraasimulu, S. Krishnakumar, D. Battalapalli, A. Vasan, M. K. Kanakasabapathy, A. Sreeram, S. Kallakuri, P. Thirumalaraju, Y. Li, S. Hua, X. G. Yu, D. R. Kuritzkes and H. Shafiee, *ACS Nano*, 2018, **12**, 5709–5718.
18 L. Zhao, Y. Liu, S. Xie, P. Ran, J. Wei, Q. Liu and X. Li, *Chem. Eng. J.*, 2020, **382**, 123041.
19 E. Blanco, H. Shen and M. Ferrari, *Nat. Biotechnol.*, 2015, **33**, 941–951.
20 S. Wang, K. Liu, Q. Zhou, C. Xu, J. Gao, Z. Wang, F. Wang, B. Chen, Y. Ye, J. Ou, J. Jiang, D. A. Wilson, S. Liu, F. Peng and Y. Tu, *Adv. Funct. Mater.*, 2021, **31**, 2009475.
21 C. Xu, S. Wang, H. Wang, K. Liu, S. Zhang, B. Chen, H. Liu, F. Tong, F. Peng, Y. Tu and Y. Li, *Nano Lett.*, 2021, **21**, 1982–1991.
22 D. Vilela, M. M. Stanton, J. Parmar and S. Sanchez, *ACS Appl. Mater. Interfaces*, 2017, **9**, 22093–22100.
23 S. Cinti, G. Valdes-Ramirez, W. Gao, J. Li, G. Palleschi and J. Wang, *Chem. Commun.*, 2015, **51**, 8668–8671.
24 K. Liu, J. Ou, S. Wang, J. Gao, L. Liu, Y. Ye, D. A. Wilson, Y. Hu, F. Peng and Y. Tu, *Appl. Mater. Today*, 2020, **20**, 100694.
25 T. Maric, V. Adamakis, Z. Zhang, C. Milian-Guimera, L. H. E. Thamdrup, E. Stamate, M. Ghavami and A. Boisen, *Small*, 2023, **19**, e2206330.
26 K. Liu, Q. Liu, J. Yang, C. Xie, S. Wang, F. Tong, J. Gao, L. Liu, Y. Ye, B. Chen, X. Cai, Z. Liu, Z. Li, F. Peng and Y. Tu, *ACS Nano*, 2023, **17**, 300–311.
27 F. Mou, C. Chen, H. Ma, Y. Yin, Q. Wu and J. Guan, *Angew. Chem., Int. Ed.*, 2013, **52**, 7208–7212.
28 S. S. Das, S. Erez, E. Karshalev, Y. Wu, J. Wang and G. Yossifon, *ACS Appl. Mater. Interfaces*, 2022, **14**, 30290–30298.
29 B. E. de Avila, P. Angsantikul, J. Li, M. Angel Lopez-Ramirez, D. E. Ramirez-Herrera, S. Thamphiwatana, C. Chen, J. Delezuk, R. Samakapiruk, V. Ramez, M. Obonyo, L. Zhang and J. Wang, *Nat. Commun.*, 2017, **8**, 272.
30 E. Karshalev, Y. Zhang, B. Esteban-Fernandez de Avila, M. Beltran-Gastelum, Y. Chen, R. Mundaca-Uribe, F. Zhang, B. Nguyen, Y. Tong, R. H. Fang, L. Zhang and J. Wang, *Nano Lett.*, 2019, **19**, 7816–7826.
31 Z. Wang, S. Wang, K. Liu, D. Fu, Y. Ye, J. Gao, L. Liu, D. A. Wilson, Y. Tu and F. Peng, *Appl. Mater. Today*, 2020, **21**, 100839.
32 Y. Feng, X. Chang, H. Liu, Y. Hu, T. Li and L. Li, *Appl. Mater. Today*, 2021, **23**, 101026.
33 F. Soto, D. Kupor, M. A. Lopez-Ramirez, F. Wei, E. Karshalev, S. Tang, F. Tehrani and J. Wang, *Angew. Chem., Int. Ed.*, 2020, **59**, 3480–3485.
34 D. Rojas, B. Jurado-Sanchez and A. Escarpa, *Anal. Chem.*, 2016, **88**, 4153–4160.
35 C. Chen, E. Karshalev, J. Guan and J. Wang, *Small*, 2018, **14**, e1704252.
36 A. M. Pourrahimi and M. Pumera, *Nanoscale*, 2018, **10**, 16398–16415.
37 R. F. Ismagilov, A. Schwartz, N. Bowden and G. M. Whitesides, *Angew. Chem., Int. Ed.*, 2002, **41**, 652–654.
38 T. R. Kline, W. F. Paxton, T. E. Mallouk and A. Sen, *Angew. Chem. Int. Ed. Engl.*, 2005, **44**, 744–746.
39 M. Safdar, O. M. Wani and J. Janis, *ACS Appl. Mater. Interfaces*, 2015, **7**, 25580–25585.
40 R. Dong, Y. Hu, Y. Wu, W. Gao, B. Ren, Q. Wang and Y. Cai, *J. Am. Chem. Soc.*, 2017, **139**, 1722–1725.
41 A. Iino, K. Suzuki, M. Kasuga, M. Suzuki and T. Yamanaka, *Ultrasonics*, 2000, **38**, 54–59.
42 N. Mano and A. Heller, *J. Am. Chem. Soc.*, 2005, **127**, 11574–11575.
43 B. J. Toebes, L. K. E. A. Abdelmohsen and D. A. Wilson, *Polym. Chem.*, 2018, **9**, 3190–3194.
44 F. Mou, C. Chen, Q. Zhong, Y. Yin, H. Ma and J. Guan, *ACS Appl. Mater. Interfaces*, 2014, **6**, 9897–9903.
45 W. Gao, X. Feng, A. Pei, Y. Gu, J. Li and J. Wang, *Nanoscale*, 2013, **5**, 4696–4700.
46 S. Cambray, M. Ibarz, M. Bermudez-Lopez, M. Marti-Antonio, M. Bozic, E. Fernandez and J. M. Valdivielso, *Nutrients*, 2020, **12**, 1–12.
47 B. A. Ryan and C. S. Kovacs, *Semin Fetal Neonatal Med*, 2020, **25**, 101062.
48 R. Salehidoost, G. Taghipour Boroujeni, A. Feizi, A. Aminorroaya and M. Amini, *Sci. Rep.*, 2022, **12**, 18209.
49 C. Yang, S. Wu, Y. Lan, S. Chen, D. Zhang, Y. Wang, Y. Sun, W. Liao and L. Wang, *Biol. Trace Elem. Res.*, 2023, **201**, 4625–4636.
50 Z. L. Nie, Z. M. Wang, B. Zhou, Z. P. Tang and S. K. Wang, *Nutr Metab Cardiovasc Dis*, 2013, **23**, 169–176.
51 N. E. Saris, E. Mervaala, H. Karppanen, J. A. Khawaja and A. Lewenstam, *Clin. Chim. Acta*, 2000, **294**, 1–26.
52 R. Fritzen, A. Davies, M. Veenhuizen, M. Campbell, S. J. Pitt, R. A. Ajjan and A. J. Stewart, *Nutrients*, 2023, **15**, 2355.
53 J. A. Maier, G. Pickering, E. Giacomoni, A. Cazzaniga and P. Pellegrino, *Nutrients*, 2020, **12**, 2660.
54 R. Nicoll, K. Gerasimidis and E. Forrest, *Alcohol Alcohol*, 2022, **57**, 275–282.
55 Y. Yang, C. He, E. Dianyu, W. Yang, F. Qi, D. Xie, L. Shen, S. Peng and C. Shuai, *Mater. Des.*, 2020, **185**, 108259.

56 N. T. Kirkland and N. Birbilis, *Magnesium Biomaterials*, 2014, ch. 4, pp. 73–94, DOI: 10.1007/978-3-319-02123-2_4.
57 Z. G. Wu, J. X. Li, B. E. F. de Avila, T. L. Li, W. W. Gao, Q. He, L. F. Zhang and J. Wang, *Adv. Funct. Mater.*, 2015, **25**, 7497–7501.
58 D. Fang, S. Tang, Z. Wu, C. Chen, M. Wan, C. Mao and M. Zhou, *Biosens. Bioelectron.*, 2022, **217**, 114682.
59 Q. Chen, W. Guo, D. Fang, T. Li, L. Chen, C. Mao, M. Wan and J. Shen, *Sens. Actuators, B*, 2023, **390**, 133933.
60 B. Jurado-Sanchez, M. Pacheco, J. Rojo and A. Escarpa, *Angew. Chem., Int. Ed.*, 2017, **56**, 6957–6961.
61 J. Li, S. Thamphiwatana, W. Liu, B. Esteban-Fernandez de Avila, P. Angsantikul, E. Sandraz, J. Wang, T. Xu, F. Soto, V. Ramez, X. Wang, W. Gao, L. Zhang and J. Wang, *ACS Nano*, 2016, **10**, 9536–9542.
62 B. Esteban-Fernandez de Avila, M. A. Lopez-Ramirez, R. Mundaca-Uribe, X. Wei, D. E. Ramirez-Herrera, E. Karshalev, B. Nguyen, R. H. Fang, L. Zhang and J. Wang, *Adv. Mater.*, 2020, **32**, e2000091.
63 R. Mundaca-Uribe, E. Karshalev, B. Esteban-Fernandez de Avila, X. Wei, B. Nguyen, I. Litvan, R. H. Fang, L. Zhang and J. Wang, *Adv. Sci.*, 2021, **8**, 2100389.
64 R. Mundaca-Uribe, M. Holay, A. Abbas, N. Askarinam, J. S. Sage-Sepulveda, L. Kubiatowicz, R. H. Fang, L. Zhang and J. Wang, *ACS Nano*, 2023, **17**, 9272–9279.
65 G. Zhao and M. Pumera, *Nanoscale*, 2014, **6**, 11177–11180.
66 L. Cai, D. Xu, Z. Zhang, N. Li and Y. Zhao, *Research*, 2023, **6**, 0044.
67 J. Li, P. Angsantikul, W. Liu, B. Esteban-Fernández de Ávila, S. Thamphiwatana, M. Xu, E. Sandraz, X. Wang, J. Delezuk, W. Gao, L. Zhang and J. Wang, *Angew. Chem., Int. Ed.*, 2017, **56**, 2156–2161.
68 Q. Song, X. Ding, Y. Liu, W. Liu, J. Li, B. Wang and Z. Gu, *Appl. Mater. Today*, 2023, **31**, 101779.
69 X. Wei, M. Beltran-Gastelum, E. Karshalev, B. Esteban-Fernandez de Avila, J. Zhou, D. Ran, P. Angsantikul, R. H. Fang, J. Wang and L. Zhang, *Nano Lett.*, 2019, **19**, 1914–1921.
70 K. Xiong, L. Xu, J. Lin, F. Mou and J. Guan, *Research*, 2020, **2020**, 1–12.
71 A. A. Solovev, Y. Mei, E. Bermudez Urena, G. Huang and O. G. Schmidt, *Small*, 2009, **5**, 1688–1692.
72 F. Zhang, R. Mundaca-Uribe, H. Gong, B. Esteban-Fernandez de Avila, M. Beltran-Gastelum, E. Karshalev, A. Nourhani, Y. Tong, B. Nguyen, M. Gallot, Y. Zhang, L. Zhang and J. Wang, *Adv. Mater.*, 2019, **31**, e1901828.
73 J. Zhou, E. Karshalev, R. Mundaca-Uribe, B. Esteban-Fernandez de Avila, N. Krishnan, C. Xiao, C. J. Ventura, H. Gong, Q. Zhang, W. Gao, R. H. Fang, J. Wang and L. Zhang, *Adv. Mater.*, 2021, **33**, e2103505.
74 J. Li, V. V. Singh, S. Sattayasamitsathit, J. Orozco, K. Kaufmann, R. Dong, W. Gao, B. Jurado-Sanchez, Y. Fedorak and J. Wang, *ACS Nano*, 2014, **8**, 11118–11125.
75 J. A. Delezuk, D. E. Ramirez-Herrera, B. Esteban-Fernandez de Avila and J. Wang, *Nanoscale*, 2017, **9**, 2195–2200.
76 L. Kong, N. Rohaizad, M. Z. M. Nasir, J. Guan and M. Pumera, *Anal. Chem.*, 2019, **91**, 5660–5666.
77 H. Yuan, X. Liu, L. Wang and X. Ma, *Bioactive Mater.*, 2021, **6**, 1727–1749.
78 S. Fu, X. Zhang, Y. Xie, J. Wu and H. Ju, *Nanoscale*, 2017, **9**, 9026–9033.
79 Y. Yang, X. Arqué, T. Patiño, V. Guillerm, P.-R. Blersch, J. Pérez-Carvajal, I. Imaz, D. Maspoch and S. Sánchez, *J. Am. Chem. Soc.*, 2020, **142**, 20962–20967.
80 M. Valles, S. Pujals, L. Albertazzi and S. Sánchez, *ACS Nano*, 2022, **16**, 5615–5626.
81 B. R. E. Smith, C. M. Njardarson and T. Jon, *J. Med. Chem.*, 2014, **57**, 9764–9773.
82 N. Sezer, Z. Evis, S. M. Kayhan, A. Tahmasebifar and M. Koç, *J. Mag. Alloys*, 2018, **6**, 23–43.
83 D. Ramanathan, L. Huang, T. Wilson and W. Boling, *Med. Gas Res.*, 2023, **13**, 94–98.
84 Z. Wu, L. Li, Y. Yang, P. Hu, Y. Li, S. Y. Yang, L. V. Wang and W. Gao, *Sci Robot*, 2019, **4**, eaax0613.
85 L. Kong, C. Chen, F. Mou, Y. Feng, M. You, Y. Yin and J. Guan, *Part. Part. Syst. Charact.*, 2019, **36**, 1800424.
86 Y. Ge, M. Liu, L. Liu, Y. Sun, H. Zhang and B. Dong, *Nanomicro Lett*, 2016, **8**, 157–164.
87 D. A. Uygun, B. Jurado-Sánchez, M. Uygun and J. Wang, *Environ. Sci.: Nano*, 2016, **3**, 559–566.